Microbial degradation of a widely used model polyethylene is restricted to medium- and long-chain alkanes and their oxidized derivatives

Ronja Marlonsdotter Sandholm[1], Gordon Jacob Boehlich[1], Ørjan Dahl[1], Ravindra R. Chowreddy[2], Anton Stepnov[1], Gustav Vaaje-Kolstad[1*] and Sabina Leanti La Rosa[1*]

[1]Faculty of Chemistry, Biotechnology and Food Science, Norwegian University of Life Sciences, Ås, Norway

[2]Norner Research AS, Porsgrunn, Norway

*Corresponding author: sabina.leantilarosa@nmbu.no and gustav.vaaje-kolstad@nmbu.no

Running title: Microbial processing of a model polyethylene

Keywords: polyethylene, polyethylene-like wax, soil microbial communities, alkanes, ketones

Abstract

Plastics are widely used materials, yet their chemical stability hinders biodegradation, exacerbating pollution on a global scale. Soils contaminated with plastic may foster microbes adapted to degrade plastics or plastic derivatives, and these organisms and their enzymes offer promising avenues for the development of biotechnological recycling strategies. Here, two microbial communities originating from soil collected at a plastic-contaminated landfill in Norway were enriched to select for bacteria involved in the decomposition of a commonly used, model polyethylene (PE; weight average molecular weight (M_w) ~4000 g/mol). We leveraged genome-resolved metatranscriptomics to identify active population affiliated with *Acinetobacter guillouiae* and *Pseudomonas* sp., showing a suite of upregulated genes (including those encoding alkane 1-monooxygenases, flavin-containing monooxygenases FMOs, cytochrome P450 monooxygenases) with functions compatible with degradation of oxidized products as well as medium- and long-chain hydrocarbons. Strikingly, spectroscopic, spectrometric and chromatographic analyses revealed the unexpected presence of medium- and long-chain alkanes and 2-ketones in the model PE substrate, preventing the erroneous conclusion that the community was interacting with the polymeric component. Consistently, only alkanes and 2-ketones with chain length of 10-35 were selectively degraded by an *A. guillouiae* isolate, as confirmed by proteomics analyses and substrate characterization following bacterial growth. Besides extending the knowledge on the enzymatic basis for degradation of PE-derivatives in soil-associated microbial systems, our results provide an advanced compositional characterization of a widely used model "PE" material, while offering valuable insight to support future studies aimed at unequivocally identifying organisms and their enzymes implicated in PE transformation.

Introduction

Plastics are synthetic materials composed primarily of long-chain polymers derived from petrochemicals. Plastics have become integral to everyday life due to their light weight, durability, electrical insulation, moldability, and cost-effective manufacturing [1]. As a consequence, global production has surged from 464 million tons per year in 2020 to a projected 804 million tons per year by 2050 [2]. Polyethylene (PE) is the most extensively manufactured plastic, constituting approximately 36% of global plastic production [3]. It is a nonpolar, partially crystalline polymer characterized by its high chemical resistance, low density, and excellent electrical insulation. PE is commonly classified as low-density polyethylene (LDPE), known for its flexibility and transparency, and high-density polyethylene (HDPE), being more rigid and dense [4].

PE-based plastics produced worldwide are either recycled, incinerated or sent to landfills. These methods are largely inefficient and energy intensive, with landfilling in particular leading to accumulation of plastic materials with impact on the surrounding environment [5,6]. In addition, the mechanical recycling of PE decreases the quality of the material due to thermo-oxidation, crosslinking and chain functionalization [7]. In the absence of efficient mechano-chemical processes that facilitate reuse of PE, there is an urgent need to explore biological approaches capable of efficiently degrading or transforming plastic waste, thereby enhancing recycling and mitigating its environmental accumulation and impact. PE-based plastics dispersed in landfill and forest soils are subjected to prolonged exposure to molecular oxygen, water, sunlight and UV radiation. These factors can trigger chemical reactions leading to the introduction of polar functional groups (e.g., carbonyl and hydroxyl) onto the polymer backbone, thus rendering PE more accessible to depolymerization, providing a unique setting for microbial adaptation [8]. Therefore, samples from landfills and soil originating from plastic-polluted areas may serve as rich reservoirs of bacteria that have evolved the ability to exploit this novel nutrient niche [9].

To address the plastic pollution challenge, plastic-degrading microorganisms and their enzymes offer promising avenues for the development of biotechnological recycling strategies. In recent years, a multitude of studies have indicated that bacteria belonging to the genera *Acinetobacter*, *Pseudomonas*, *Rhodococcus*, *Brevibacillus*, *Aneurinibacillus* and *Bacillus*, among others [10-17] possess capabilities to depolymerize PE through different enzyme systems. These potential enzymes belong to various oxidoreductase families, such as alkane hydroxylases, laccases, manganese peroxidases and monooxygenases [9]. Despite these claims, the mechanism by which PE can be degraded by microbes in natural environments remains controversial [18]. Indeed, interpretation of data on the depolymerization and metabolization of PE is often complicated by the lack of appropriate controls, use of unspecific analytical techniques (e.g., microscopy or

infrared spectroscopy), and by the reliance on non-characterized model plastics, which may contain metabolizable additives and oligomers [19].

In this study, we used a multi-omics approach to functionally characterize two microbial communities enriched on a low molar mass polyethylene-like wax (PELW), a commonly used model substrate in PE studies. The microbial communities were sourced from a plastic-contaminated landfill in Norway, and therefore they faced a prolonged exposure to plastic, including PE, prior to the experiment. We report the isolation of a bacterium, *A. guillouiae* FS11 able to grow on PELW, and employed proteomics to identify enzymes involved in the depolymerization of components derived from the PELW. Furthermore, a combined analytical approach showed that the PELW was substantially oxidized "out of the box", a property not noted by the manufacturer, with consequence on its microbial accessibility. Besides extending the knowledge on the enzymatic basis for degradation of PE-derivatives in soil-associated microbial systems, our findings also offer a cautionary perspective on the increasing number of studies claiming enzymatic degradation of materials with insufficient compositional characterization.

Material and methods

Sample collection and microbial profiling using 16S rRNA amplicon sequencing

Soil was collected on the 1st of November 2022 from a plastic contaminated landfill in Finnskogen (Flisa, Norway). under a permit of the regional authority of Flisa Municipality. At sampling, large amounts of macroplastic items were present on the surface and buried, having accumulated at this site since the 1970s-1980s without removal. Two locations were sampled: S1 (~5 cm topsoil; 60°40'32.32''N, 12°6'18.98''E) and S2 (~15 cm subsoil; 60°40'32.71''N, 12°6'19.07''E). The original S1 and S2 samples were sent to DNASense ApS (Aalborg, Denmark) for 16S rRNA amplicon sequencing. Detailed information for DNA extraction, library preparation, sequencing and data analysis is provided in the Supplementary Material.

Substrates and growth conditions

PE powder from Sigma-Aldrich (cat. number 427772; weight average molecular weight (M_w) ~4000 g/mol, number average molecular weight (M_n) ~1700 g/mol), was used as a model commercial substrate. Because its M_w is far below that of conventional polyethylene (> 100,000 g/mol), we designate the material as a polyethylene-like wax (PELW) to distinguish it from high-M_w, "common" polyethylene. Triacontane (C30) and tetracontane (C40) were obtained from Sigma-Aldrich (cat. number 263842 and 87087). D-glucose and sodium acetate were purchased from VWR (cat. number 0188-2.5KG) and Sigma-Aldrich (cat. number S2378), respectively. LDPE

101 granules from Borealis (grade FT5230) milled to powder with 200-300 µm particle diameter.
102 Unless stated otherwise, cultures were grown using M9 minimal salts medium (MM)
103 supplemented with a single carbon source [20]. Microbial growth was determined
104 spectrophotochemically by measuring optical density at 600 nm (OD600).

105 Selective enrichment of soil samples on PELW and alkanes

106 The sequential enrichment protocol was initiated by inoculating MM containing 10 mg/mL PELW
107 as a sole carbon source with soil from S1 and S2. These primary cultures were incubated for 10
108 days, then 100 µL were transferred to 20 mL of fresh MM with PELW to obtain secondary cultures.
109 Tertiary cultures were prepared by inoculating 100 µL of a secondary culture into three separate
110 conditions: 20 mL of fresh MM containing PELW (resulting in the cultures indicated as S1PELW
111 and S2PELW), 20 mL of MM supplemented with 10 mg/mL of C30 (S1C30 and S2C30), and 20 mL
112 of MM supplemented with 10 mg/mL of C40 (S1C40 and S2C40). Incubation conditions in all
113 enrichment phases were 30°C with 200 rpm agitation. At each enrichment step, two controls (i.e.,
114 MM without substrate or MM without any microbial source) were also set up and subjected to the
115 same conditions.

116 Shotgun sequencing and assembly of metagenomes

117 Samples from the tertiary communities S1PELW, S2PELW, S1C30, S2C30, S1C40 and S2C40 were
118 collected in the early stationary phase (**Fig. S2**) by pelleting at 15,000 G for 10 min. Pellets were
119 resuspended in 800 µL Solution CD1 from the DNeasy® PowerSoil® Pro kit (QIAGEN, ID: 47014)
120 and DNA was extracted according to the manufacturer's instructions. DNA size was selected using
121 a Short Read Eliminator XS kit (PacBio, PN: 102-208-200). DNA was quantified using Qubit™
122 dsDNA Broad Range Assay (Invitrogen) on a Qubit™ 1.0 fluorometer. DNA size was assessed using
123 gel electrophoresis, and purity was evaluated using a NanoDrop™ One Microvolume UV-Vis
124 spectrophotometer (ThermoFisher Scientific). Sequencing libraries were prepared using the
125 Native Barcoding kit SQK-NBD114.24 (Oxford Nanopore Technologies, UK) following the
126 manufacturer's instructions. S1PELW and S2PELW libraries were pooled, as were S1C30 with
127 S2C30, and S1C40 with S2C40. Each pooled sample was then sequenced on a separate R10.4 flow
128 cell on a MinION device (Oxford Nanopore Technologies, UK). POD5 files were base-called and
129 demultiplexed with Dorado v0.5.0 [21], using the super-accurate model (config:
130 dna_r10.4.1_e8.2_400bps_sup@v4.3.0).

131 The snakemake wrapper Aviary v0.9.1 was used to recover MAGs [22]. Low-quality MAGs,
132 defined according to the MiMAG standards [23] were removed from the dataset. MAGs were
133 taxonomically classified using GTDB-Tk [24] with the GTDB database release 220. Functional
134 annotation of the bacterial genomes was performed with DRAM v1.4.6 [25] with the following

135 databases: Uniref90, PFAM-A, KOfam and dbCAN-V10 (all downloaded in January 2024). Figures
136 were created using R v4.3.3 [26] and ggplot2 v3.5.1 [27].

137 Metatranscriptomic analysis

138 Samples from the tertiary communities S1PELW, S2PELW, S1C30, S2C30, S1C40 and S2C40 were
139 collected by pelleting at 15,000 G at 4 °C in mid-exponential phase. Pelleted samples were shipped
140 to Novogene (Cambridge, UK) for extraction and sequencing of metaRNA. Detailed information
141 for RNA extraction and sequencing is provided in the Supplementary Material. Raw
142 metatranscriptomic reads were quality checked using FastQC v0.12.1 [28] filtered using fastp
143 v0.23.4 (`-q 20`) [29] and ribosomal RNA removed from the dataset using SortMeRNA v4.3.6 [30].
144 The filtered metatranscriptomic dataset was pseudo-aligned against the recovered MAGs using
145 Kallisto v0.48.0 [31]. Transcripts per million (TPM) values were $\log_2$-transformed. Genes with
146 transcripts in 2 out of 3 replicates were kept. The remaining missing values were imputed from a
147 normal distribution (width of 0.3 and down shifted 1.8 standard deviations from the original
148 distribution). To find differentially expressed genes, a paired t-test ($p \leq 0.05$) was preformed
149 using Rstatix v0.7.2 comparing the data from C30, C40 or PELW to a glucose control [32]. Figures
150 were generated using R v4.3.3 [26] packages ggplot2 v3.5.1, cowplot v1.1.3 [33] and ggrepel
151 v0.9.5 [34].

152 Isolation of *Acinetobacter guillouiae* FS11 and proteomic analysis

153 *Acinetobacter guillouiae* was isolated from the S1PELW tertiary community following selection
154 on MM containing 10 mg/mL PELW and Luria Bertani (LB, Sigma-Aldrich, L3522) plates
155 supplemented with 50 µg/mL kanamycin sulfate (Gibco, 11815-032). Detailed information for
156 the identification of *A. guillouiae* FS11 is provided in the Supplementary Material. To obtain
157 samples for proteomic analysis, *A. guillouiae* FS11 was cultured in triplicates in MM
158 supplemented with either 10 mg/mL PELW, 10 mg/mL C30 or 2% v/v sodium acetate. Three
159 samples types were collected in the mid-exponential phase (**Fig. S4**): planktonic cells, surface
160 biofilm attached to PELW, and secreted proteins. Detailed information for protein extraction,
161 trypsin digestion, and mass spectrometry analysis is provided in the Supplementary Material.

162 Analysis of mass spectrometry data was done using FragPipe v21.1
163 (https://fragpipe.nesvilab.org/), with MSFragger v4.0 [35], IonQuant v1.10.12 [36], Philosopher
164 v5.1.0 [37]. A sample specific database consisting of the *A. guillouiae* FS11 proteome (4615
165 proteins) was used. The final database was supplemented with common contaminants (e.g.,
166 human keratin, bovine serum albumin and casein) and contained reverse entries of all library
167 sequences. Carbamidomethylation was used as a fixed modification, while oxidation of
168 methionine and protein N-terminal acetylation were added as variable modifications. Trypsin

169 was used as a digestive enzyme, with maximum one missed cleavage allowed. For Label-Free-
170 Quantification (LFQ), IonQuant was applied with FDR-controlled match-between-runs (MBR)
171 enabled. The LFQ intensity values were log-transformed, and a protein was considered "present"
172 if it was detected in at least two of the three biological replicates in at least one condition. Missing
173 values were imputed from a normal distribution. Differential abundance analysis was performed
174 using a paired t-test ($p \leq 0.05$) in Rstatix v0.7.2 [32] in R v4.3.3 [26]. Figures were generated
175 using the packages ggplot2 v3.5.1 [38], cowplot v1.1.3 [33] and R v4.3.3 [26].

176 Protein structure prediction

177 3D structural models of the top 50 most abundant proteins in the *A. guillouiae* FS11 PELW-
178 proteome were generated using AlphaFold3 [39]. Structure similarity searches were performed
179 using FoldSeek [40]. Molecular images, with computation of surface potential, were generated
180 using UCSF ChimeraX v1.10 [41].

181 Microscopy

182 Experimental samples consisted of 10 mg/mL PELW derived from MM inoculated with S1PELW
183 or S2PELW soil communities, or *A. guillouiae* FS11, while control samples consisted of 10 mg/mL
184 PELW derived from MM without any microbial source. Scanning electron microscopy (SEM)
185 analysis was conducted using a Hitachi SU5000 microscope (Hitachi High-Technologies
186 Corporation, Japan). The specimens for SEM analysis were prepared by spreading powdered
187 PELW samples on an EM-Tec CT12 conductive double sided adhesive carbon tab (Delta
188 Microscopies, France) and by sputter coating with Platinum with Cressington 208 HR sputter
189 coater (Cressington Scientific Instruments, England). For sputter coating, 20 mA sputter current
190 for 30 seconds and sample holder with tilt and rotation was utilized. The Platinum coated
191 specimens were investigated for SEM under high vacuum mode with SE detector at an accelerated
192 voltage between 1.5 – 3 kV and working distance about 10 mm.

193 Substrate characterization

194 Fourier-transform infrared spectroscopy

195 The FT-IR spectrum of the PELW and pure LDPE (FT5230, Borealis, Austria) was acquired with
196 a Spectrum Two FT-IR spectrometer (PerkinElmer, Waltham, MA, USA) equipped with a Quest
197 ATR (attenuated total reflectance) sampling module (Specac Ltd, Orpington, United Kingdom).
198 The signals were obtained with 4 cm^{-1} spectral resolution (8 consecutive readings per
199 measurement) in the 4000-550 cm^{-1} range using Spectrum IR software (PerkinElmer, Waltham,
200 MA, USA). The carbonyl index was determined by calculating the ratio of the absorbance peak at
201 1715 cm^{-1} to the reference peak at 1505 cm^{-1}.

202 **Pyrolysis-gas chromatography-mass spectrometry**

203 Samples consisting of 150-250 µg of PELW or a commercial LDPE (grade 22H594; INEOS Olefins
204 Switzerland), were placed in a deactivated stainless-steel sample cup and introduced into a multi-
205 shot EGA/PY-3030D pyrolyzer (Frontier Laboratories, Japan) coupled to a 7890N gas
206 chromatograph and a 5975 mass selective detector (Agilent Technologies, USA). The furnace
207 temperature was maintained at 550 °C and the interface between the furnace and the GC-MS
208 system was set to 300 °C. The GC injector was operated in split mode (100:1 ratio) at 300 °C. The
209 analysis of volatile products was performed using an Ultra-Alloy metal capillary column
210 containing 5 % diphenyl- and 95 % dimethylpolysiloxane stationary phase (30 m, 0.25 mm ID,
211 0.25 µm; Frontier Laboratories Ltd., Japan) using helium as carrier gas at 1 ml/min flow rate. The
212 GC oven temperature increased from 70 °C to 350 °C at 20 °C/min and maintained at 350 °C for
213 16 min. The electron ionization (70 eV) mass selective detector was operated with an ion source
214 temperature of 230 °C, interface temperature of 300 °C, and a scan range of 29-350 m/z.

215 Compound identifications were done by matching chromatograms using an F-Search in the Wiley
216 11th edition/NIST 2017 spectral library. To refine identification, spectral match scores were
217 combined with retention times to differentiate between compounds with similar spectra.

218 **^{1}H and ^{13}C nuclear magnetic resonance spectroscopy**

219 ^{1}H-NMR and ^{13}C-NMR spectra of PELW and PE wax samples were recorded at 328 K using a
220 Bruker AVANCE III HD 400 MHz instrument equipped with a BBFO room temperature probe. For
221 sample preparation, 5 mg of pristine PELW and a PE wax (Licocene 5301; Clariant AG,
222 Switzerland) were suspended in 0.5 mL $CDCl_3$ and transferred to a 5 mm Norell® Sample Vault
223 Series™ NMR tube. Heating these samples to 328 K gave clear solutions. Chemical shifts are
224 reported in ppm with the solvent signals (7.26 ppm for ^{1}H/ 77.16 ppm for ^{13}C) as internal
225 standard. The following pulse programs where used: "`zg30`" for ^{1}H, "`deptqgpsp.2`" for DEPTQ-
226 ^{13}C, "`hsqcetgpsi2`" for HSQC and "`hmbcetgpl3nd`" for HMBC Phase contrast and scanning
227 electron microscopy.

228 **Size exclusion chromatography and gas chromatography-mass spectrometry**

229 Three types of samples (untreated PELW, PELW incubated in MM without any microbial source
230 and PELW incubated in MM with *A. guillouiae* FS11) were prepared to assess the impact of *A.*
231 *guillouiae* FS11 on substrate composition for subsequent GC-MS and SEC analysis (see
232 Supplementary Methods). The weight average molecular mass (M_w), number average molar mass
233 (M_n), and the molecular weight distribution in the PELW samples were determined using a GPC-
234 IR5 system (Polymer Char, Spain) equipped with four PLgel 20 µm MIXED-A columns (Agilent
235 Technologies, USA). Approximately 4 mg of a pure LDPE (FT5230, Borealis, Austria), PELW and a

236 PE wax (Licocene™ 5301; Clariant AG, Muttenz, Switzerland) were dissolved in 8 ml of 1,2,4-
237 trichlorobenzene by mixing at 160°C for 3 hours. For SEC analysis, 200 µl of the samples were
238 injected into the SEC system. The analysis was performed at 150 °C using a high-sensitivity
239 infrared detector and 1,2,4-trichlorobenzene as a mobile phase (1.0 mL/min flow rate).
240 Polystyrene standards with a narrow M_w distribution and M_{peak} (most abundant M_w in the sample)
241 in the range of 1140 – 7,500,000 g/mol (Agilent Technologies, USA) were used for calibration.

242 For GC-MS, extraction of low molecular weight compounds was conducted from approximately
243 100 mg of PELW by mixing with 3 mL of ethyl acetate in PTFE/Silicone septum sealed glass vials.
244 The vials were heated at 95°C for 1.5 hours and the liquid fraction filtered through a 0.2 µm Teflon
245 syringe filter and subjected to GC-MS analysis.

246 GC-MS analysis was carried out using an Agilent 6890N gas chromatograph (Agilent Technologies,
247 Inc., USA) coupled to an Agilent 5973 Network Mass Selective Detector (Agilent Technologies,
248 USA) and a Gerstel MPS2 Autosampler (GERSTEL GmbH & Co.KG, Germany). The gas
249 chromatograph was equipped with 30 m Zebron ZB-5MSPlus column having a 250 µm internal
250 diameter and 0.25 µm coating thickness (Phenomenex, USA). The temperature of the column
251 increased from 60 °C to 300 °C at a heating rate of 10 °C per minute with a total run time of 45
252 minutes. Helium with a purify grade of 6.0 was used as a carrier gas at a flow rate of 3 mL/minute.
253 The mass spectrometer was operated in electron ionization mode at 70 eV. Mass spectra and the
254 total ion chromatograms were obtained by automatic scanning a mass range (m/z) of 33-720.
255 Three runs per sample (n=3) were performed. The volatile components were identified by
256 comparing the mass spectrum with those available in the Wiley 11th edition/NIST 2017 spectra
257 library. Compounds were quantified by calculated response factors. Response factors were
258 calculated by using the reference compounds BHT (butylated hydroxytoluene) and Tinuvin® 120
259 (2',4'-Di-tert-butylphenyl 3,5-di-tert-butyl-4-hydroxybenzoate), as they give differences in the
260 responses between lower and higher molecular weight components.

261 Results

262 Microbial communities from a plastic-enriched landfill include 263 metabolic active bacteria that grow on PELW, but not on LDPE

264 As part of an effort to discover and characterize microbes and their enzymes able to degrade LDPE
265 and PELW, soil samples were collected from a landfill that has been exposed to plastic waste since
266 the 1970s. Samples were collected from two different locations and depths and subjected and
267 subjected to 16S rRNA gene amplicon sequencing, which revealed species previously associated
268 with the degradation of various plastics and alkanes (**Supplementary results and Fig. S1**).

269 An enrichment protocol by sequential passaging was employed in order to select microbial
270 species specifically involved in the degradation of LDPE, PELW and two distinct alkanes
271 (triacontane and tetracontane). The two alkanes were used as substrates since they may trigger
272 the catabolic systems also used for PE degradation. Cultures showed growth on PELW,
273 triacontane and tetracontane (**Fig. S2**). In contrast, no growth was observed when LDPE was
274 provided as the sole substrate.

275 Long-read metagenomic sequencing of the enrichment cultures yielded a total of 84 high-quality
276 and 46 medium-quality dereplicated MAGs (**Fig. S3**). The use of long-read DNA sequencing
277 ensured that 127 MAGs encoded full-length 16S rRNA genes, which enabled searches for the
278 occurrence of these bacteria in the amplicon dataset generated from the original soil samples. At
279 a 97% identity cut-off when comparing the 16S rRNA sequences derived from the MAGs in the
280 enrichment cultures to OTUs, 125 of 130 MAGs were detected in the original soil microbial
281 communities S1 and S2 (**Fig. 1A**). Of the undetected MAGs, 3 of 5 MAGs were missing a 16S rRNA
282 gene. The S1PELW and S1C30 enrichments were characterized by the dominance of MAG107
283 (55.81%) and MAG13003 (62.81%), respectively, both taxonomically identified as *Acinetobacter*
284 *guillouiae* (**Fig. 1B, Table S1A**). *A. guillouiae* was absent from the S1C40 community, suggesting
285 its limited capacity to metabolize alkanes with a chain length >30. The S2PELW and S1C40
286 consortia were characterized by a high relative abundance (42-62%) of MAGs affiliated to the
287 genus *Pseudomonas*. Scanning electron microscopy (SEM) provided an initial qualitative insight
288 into the distribution and morphological diversity of microbial cells with the ability to adhere to
289 the substrate. Species with distinct morphologies were observed in the S1PELW and S2PELW
290 communities (**Fig. 1C and 1D**). In both samples, microorganisms formed dense and slimy clusters
291 on the PE particles, resembling biofilms. Additional 16S RNA amplicon sequencing of the bacteria
292 attached to the PELW surface confirmed the presence of *Acinetobacter* and *Pseudomonas*,
293 respectively, in agreement with their prevalence in the corresponding enrichment community.

294 A genome-resolved metatranscriptomics approach allowed us to identify metabolically active
295 MAGs and their upregulated genes in response to PELW, triacontane and tetracontane to a control
296 where glucose was used as the sole carbon source. Intriguingly, transcripts abundance (relative
297 to the total TPMs) for each MAG in the communities did not always reflect their abundance in the
298 enrichments (**Fig. 1B**). In the S1PELW community, the most abundant, and most active MAG, was
299 MAG107 (*A. guillouiae*) (**Fig. 1B**). The second most active MAGs, MAG108 (*Pseudomonas*) and
300 MAG134 (*Aeromonas*), were not prevalent MAGs in the enrichment community (3.2% and 0.83%,
301 respectively). As for the S2PELW community, MAG238 and MAG206 (*Pseudomonas*) were highly
302 active, with MAG238 not being the most predominant *Pseudomonas* in the enrichment (8.33%).
303 This observation applies to all the enrichments, where the most abundant MAGs were not
304 necessarily the most active, highlighting the need for functional data to accurately characterize

305 true metabolism of substrates by microbial community members that may be dormant or slow
306 growers.

307 Closer examination of the metatranscriptome showed that in the S1PELW community MAG107
308 (*A. guillouiae*) accounted for all upregulated genes associated with the alkane terminal oxidation
309 pathway including those coding for an alkane 1-monooxygenase (*alkM*) and the electron-transfer
310 components rubredoxin (*rubB*) (**Fig. 2A**). In addition, several genes encoding flavin-containing
311 monooxygenases (FMOs) were upregulated. While MAG107 appears to be the principal driver of
312 substrate degradation, other MAGs including MAG134 (*Aeromonas aquatica*) and MAG108
313 (*Pseudomonas* sp.) displayed upregulated genes coding for enzymes involved in β-oxidation of
314 fatty acids (**Table S1B**). In the S2PELW community, several MAGs exhibited upregulated genes
315 encoding enzymes contributing to alkane degradation (**Fig. 2B**). Here, MAG238 (*Pseudomonas*
316 sp002029345), MAG206 (*Pseudomonas fluorescens*) and MAG234 (*Pseudomonas veronii*) show
317 increased expression of genes coding for aldehyde dehydrogenases (*aldH*) and alcohol
318 dehydrogenases (*yiaY*, *adhP*, *ADH* and *exaA*). In this community, genes coding for cytochrome
319 P450s (CYPs), which have been associated with both terminal and subterminal hydroxylation of
320 alkanes [42], were upregulated in MAG238, suggesting its potential role as main degrader (**Table**
321 **S1C**).

322 The S1C30 community was dominated by MAG13003 (*A. guillouiae*), which exhibited
323 upregulation across the full suite of genes involved in alkane degradation (**Fig. 2C**). In addition,
324 MAG13023 (*Achromobacter* sp.) upregulated genes encoding alcohol dehydrogenases and
325 aldehyde dehydrogenases, as well as a CYP, suggesting a potential role in alkane transformation.
326 Upregulated genes for FMOs were detected in MAG13003, potentially oxidizing 2-ketones
327 generated by CYP's activity. Although MAG13023 was not one of the most active MAGs in the
328 community (**Fig. 2C**), this MAG and MAG13003 seem to share the role as main degraders, whereas
329 MAG13012 (*Achromobacter kerstersii*), MAG13007 (*Aeromonas aquaticia*) and MAG13006
330 (*Pseudomonas putida*) have genes in the β-oxidation pathway upregulated (**Table S1D**). In the
331 S2C30 community, MAG23002 (*Pseudomonas* sp.) showed upregulated genes in the alkane
332 degradation pathway, including *alkM*, the long-chain alkane monooxygenase *ladA* and *cyp*, as well
333 as the β-oxidation pathway, suggesting its role as main degrader (**Fig. 2D**). MAG23043 (*Kaistella*
334 *soli*) displayed upregulated genes encoding enzyme involved in the β-oxidation pathway (**Table**
335 **S1E**).

336 In the S1C40 community, MAG14012 (*Achromobacter* sp.) upregulated genes encoding a CYP, as
337 well as genes encoding enzymes involved in the full alkane degradation pathway and the β-
338 oxidation pathway were detected (**Fig. 2E, Table S1F**). Other active MAGs (MAG14015;
339 *Pseudomonas* sp, MAG14001; *A. guillouiae* and MAG14011) lacked the initial alkane hydroxylation

340 step but showed upregulation of genes coding for enzymes involved in the subsequent alkane
341 oxidation and β-oxidation pathway, as well as MAG14001 upregulated a gene coding for an FMO.
342 In the S2C40 community, MAG24005 (*P. fluorescens*) and MAG24013 (*P. veronii*) showed
343 upregulated genes coding for AlkM, LadA, with MAG24005 also upregulating a gene coding for a
344 CYP (**Fig. 2F, Table S1G**).

345 Overall, comparison of the community transcriptional response in PELW versus S1C40 and S1C30
346 revealed no upregulated genes in PELW encoding enzymes potentially capable of cleaving the C–
347 C bonds of the polymeric component.

348 PELW (Sigma-Aldrich PE) is oxidized at the chain ends

349 Many studies have reported microbial degradation of the Sigma-Aldrich low molecular mass PE
350 (i.e. catalog number 427772) [15,43-50], referred to as PELW in this study, a phenomenon
351 reproduced by our enrichment cultures (**Fig. S2**). Since we observed no growth on pristine LDPE
352 and no differentially expressed gene that could be linked to enzymes able to interact with the
353 polymeric substrate, it was of interest to perform a deeper analysis of the PELW material to
354 identify the constituents that may be responsible for sustaining microbial growth. SEC analysis
355 showed that the PELW M_w (weight average molecular mass) is ~3900 g/mol, which is similar to
356 what is reported by the manufacturer (~4000 g/mol). This is indeed substantially lower than a
357 reference LDPE, with M_w of 97 300 g/mol, and slightly lower than a PE wax (~5400 g/mol) (**Table**
358 **S2A**). To determine the putative presence of functional groups from oxidized derivatives, PELW
359 and LDPE were subjected to FTIR analysis (**Fig. 3B**). To our surprise, a strong peak at ≈1722 cm-
360 ^{1} was observed in the PELW sample corresponding to stretching of a carbonyl group in an
361 aldehyde or a ketone, accompanied by additional much weaker peaks at ≈1409 and ≈1158 cm^{-1}.
362 The LDPE sample showed no sign of oxidation. To identify the type and extent of oxidation of the
363 PELW, the polymer was analyzed by NMR. To determine the presence of ketones in the PELW,
364 and to determine the positions of the carbonyl groups, the PELW structure was elucidated using
365 one- and two-dimensional ^{1}H and ^{13}C-NMR (**Fig. 3C**). The ^{1}H-NMR spectrum displayed a large
366 singlet at 1.28 ppm, which is characteristic of the CH_2-groups within the hydrocarbon backbone
367 of PE. As expected, this peak was present in both the PE wax and the PELW samples. However,
368 additional signals from the PELW were detected between 2.00-2.50 ppm. The chemical shift of
369 these signals is typical for protons located next to carbonyls. The singlets at 2.10 and 2.12 ppm
370 are characteristic of CH_3 groups next to a carbonyl. The two triplets at 2.37 and 2.40 ppm indicate
371 CH_2 groups next to a carbonyl. The ^{1}H-^{13}C-HMBC-spectrum showed correlations from the triplet
372 at 2.40 ppm and the singlet at 2.12 ppm to a carbonyl signal at 208.7 ppm, confirming that these
373 signals stem from a methyl ketone (2-ketone). The smaller triplet at 2.37 ppm showed a
374 correlation to a carbonyl signal at 211.3 ppm, indicating this triplet stems from in-chain ketones.

375 The small singlet at 2.10 ppm showed a correlation to a carbonyl at 212.5 ppm, which stems from
376 a 2-ketone next to a branching point. At 9.77 ppm, the ^{1}H-NMR-spectrum also showed a triplet
377 just above noise level, indicating that trace amounts of aldehydes are also present. The NMR data
378 also provides means to quantify the degree of oxidation. Based on integrals in the ^{1}H-NMR-
379 spectrum, approximately 6‰ of all carbon atoms in the PE are oxidized to ketones. Of these
380 ketones, 84% are 2-ketones. The Py-GC-MS data revealed the presence of analytes in the PELW
381 sample that were not observed in the LDPE control sample (**Fig. 3D**). These peaks were identified
382 as 2-ketones between 12-32 carbons, using a reference library (**Table S2D**). GC-MS analysis
383 confirmed the presence of these small molecules by identifying hydrocarbons, including alkanes
384 with 13-35 carbons and 2-ketones with 10-34 carbons in the PELW samples (**Fig. 3E, Table S2E**).
385 The presence of short 2-ketones in the PELW introduces oxygen functionality, potentially
386 increasing the bioavailability of the plastic compared to pristine LDPE.

387 An *A. guilloiae* FS11 isolate catabolizes low molecular mass alkanes 388 and 2-ketones present in PELW

389 To gain deeper insight into the bacterial metabolism of PELW constituents, we isolated the
390 dominant species from the metagenomic analysis, namely *A. guillouiae* FS11. While not growing
391 on pristine LDPE (**Fig. 4A**), the growth of *A. guillouiae* FS11 on PELW was remarkably rapid for
392 an insoluble substrate, showing an increase in OD600 from 0.00 to 0.56 after 75 h incubation (**Fig.
393 S4**). SEC analysis of the PELW particles after bacterial growth showed a reduction of the amount
394 of alkanes smaller than ~316 g/mol (**Fig. 4B**; see the zoomed-in view). Remarkably, the
395 molecular mass distribution curve obtained for PELW after bacterial grow closely overlapped
396 with that of the negative control sample, providing no evidence for degradation of polymeric PE
397 substrate. GC-MS quantification of the PELW low molecular mass oligomers showed depletion of
398 the smallest alkanes and 2-ketones and substantial reduction in medium length oligomers (10 to
399 35 carbons in length), compared to the control samples (**Fig. 4C**). Interestingly, the PELW
400 particles that only were exposed to MM medium, also showed a partial reduction in short alkane
401 and 2-ketone oligomers (**Fig. 4C**), suggesting formation of shorter derivatives that are likely
402 easily accessible for microorganisms. Similar to the observations made for enrichment cultures
403 growing on PELW (**Fig. 1C and D**), *A. guillouiae* FS11 formed biofilms on the surface of PELW
404 particles (**Fig. 4D**).

405 *A. guillouiae* FS11 may use flavin-containing monooxygenases for 406 2-ketone conversion

407 To identify the enzymes involved in the degradation of the oligomeric alkanes and 2-ketones in
408 PELW, we conducted a proteomic analysis of secreted, planktonic and biofilm-derived proteins

409 produced by *A. guillouiae* FS11 during growth on PELW, triacontane and sodium succinate.
410 Enzymes involved in alkane degradation, putative 2-ketone degradation and β-oxidation were
411 generally more abundant under PELW conditions (**Fig. 5A**). In the biofilm-derived proteome, all
412 known enzymes involved in alkane degradation, as well as the putative enzymes involved in 2-
413 ketone oxidation were detected (**Fig. 5A**). Two LadA (LadA_3609, LadA_4534), were exclusively
414 detected in the PELW-biofilm proteome. AlkB_3757 was detected in all proteomes, except for the
415 succinate control. Finally, YiaY_433 and ALDH_4343 were among the most abundant proteins
416 detected in the PELW-associated (biofilm, planktonic and secreted) and C30 (planktonic)
417 proteomes (**Fig. 5A**), indicating that enzymes involved in the complete alkane degradation
418 pathway are active under these conditions.

419 Several differentially abundant FMOs, that may be actively transforming 2-ketones, were
420 identified in the PELW and C30 proteomes (**Fig. 5A**). These included the FMO_386, encoded by a
421 gene associated with a cluster that was confirmed via BLASTn analysis to correspond to the *sad*
422 gene cluster of *Acinetobacter sp.* strain NyZ410 [51]. FoldSeek predictions using AlphaFold3
423 models indicated that the FMO corresponds to SadD, a BVMO known to convert aliphatic ketones
424 into esters [51]. Additional FMOs were detected at high abundance either exclusively in the PELW
425 proteome (FMO_2974), or in the PELW or C30 proteome (FMO_3676, FMO_1117). All these FMOs
426 exhibit high structural and sequence similarity to characterized BVMOs (**Fig. S6, Table S1J**). The
427 presence of multiple FMOs in the proteome may reflect the need to accommodate the 2-ketones
428 of different chain lengths detected in the PELW (**Fig. 4C**), as such protein redundancy is
429 commonly considered a strategy to expand substrate range [52]. The esterases SadA_389 and
430 SadB_388, together with the carboxylesterase CES_3782, exhibited significantly higher
431 abundance in the proteomes derived from PELW and C30 compared to the control conditions
432 (**Fig. 5A**). The hydrolysis products (an alcohol and acetate) derived from the activity of these
433 enzymes can either enter the terminal alkane oxidation pathway or be converted into acetyl-CoA
434 by the Acetyl-CoA Synthetase ACS_1444, respectively (**Fig. 5A**).

435 Collectively, the detection of the enzymes described above (**Fig. 5A**), in combination with the
436 depletion of both alkanes and 2-ketones (**Fig. 4C**), indicate that the small molecules derived from
437 the PELW can be consumed through terminal alkane oxidation and 2-ketone degradation, which
438 is a shorter version of the subterminal oxidation of alkanes (**Fig. 5B**).

439 Discussion

440 Biotechnological conversion of PE to useful products like platform chemicals or microbial single
441 cell proteins is an important research area given the unfathomable amounts of PE waste available
442 and continuously accumulating on the planet. Indeed, many studies exist where PE is reported to

443 be microbially or enzymatically degraded [53,54], but few of these have been reproduced by
444 others and some attempts of reproduction have failed [55]. Recently, several cautionary articles
445 and reviews have been published that urge research to be more careful in experimental design
446 and interpretation of results [18,55,56]. One common misunderstanding arises from the use of
447 model PE substrates that do not have the properties of a typical industrial-grade PE. A very good
448 example is the PELW used in the present study, which is marketed as "PE" by the supplier (Sigma-
449 Aldrich). This product has been used in multitude of studies [15,43-50], many of which report
450 microbial PE-degradation. From a polymer chemist standpoint, the Sigma-Aldrich PE is a PE-like
451 wax due to its low M_w (~3900 g/mol), and such a polymer cannot be compared to a typical
452 commercial PE which has M_w often exceeding 100 000 g/mol, where the high molecular weight is
453 what provides the high chemical and structural robustness. Our data clearly shows that bacteria
454 like *A. guillouiae* F11, as well as microbial communities can efficiently utilize PELW as a sole
455 carbon source by metabolizing the alkane oligomers and 2-ketones present in the wax (**Fig. 4 and**
456 **Fig. S2**). In our commercial LDPE sample, no such oligomers were present (**Fig. 3**), thus neither
457 the *A. guillouiae* F11 isolate, nor the soil derived microbial communities were able to grow (**Fig.**
458 **S2 and Fig. S4**). It is not unlikely that the mechanism of PELW utilization in other studies, where
459 the PELW is mistaken for a compound that has the properties of high-molecular mass PE (even
460 referred to as LDPE at times, [43,45,47,48]), is the same as observed in our study. A second key
461 observation made in the present study is the abundant presence of 2-keto groups in the PELW
462 chains (**Fig. 3**), a feature absent from the supplier's product specification, that could increase the
463 material's biodegradability. Interestingly, we are not the first to identify oxidation of the PELW.
464 Zampolli et al. also performed GC-MS on the material (most likely a different batch) and reported
465 the presence of multiple different oxygen-containing functional, groups, including 2-ketones [49].
466 These observations suggest that it is not only the product purchased for the present study that is
467 oxidized, but possibly a larger batch of the product. Notably, FTIR analysis of two independently
468 purchased PELW samples (batch numbers MKCT5408 and MKCP961) confirmed the same
469 oxidation pattern (results not shown). Carbonyl groups can be introduced into PE, including the
470 low molecular weight fractions, through i.e. chemical [57], thermal [58] and photo-oxidation [59],
471 supporting the idea that these components are oxidation derivatives from original PELW material.

472 The mechanism by which the oligomeric alkanes and 2-ketones are consumed can give valuable
473 insight into how PE waste potentially can be enzymatically depolymerized, given that the material
474 is pretreated to reduce molecular weight, e.g. by oxidation. When searching for microorganisms
475 with the capability to depolymerize PE, or oxidized PE components and derivatives, it is
476 reasonable to focus on natural communities that have been exposed to plastic pollution over
477 many years. In this work, an enrichment experiment using an oxidized PELW was established
478 from soil communities from a landfill contaminated with weathered plastic waste. Shotgun

479 metagenomic profiling showed that *Acinetobacter* and *Pseudomonas* spp. became abundant in the
480 enrichment cultures on PELW, triacontane and tetracontane (**Fig. 1B**). Members of the genera
481 *Pseudomonas* [60,61] and *Acinetobacter* [52,62] are some of the most studied alkane degrading
482 microorganisms, and have been proposed to be able to adhere and/or degrade PE [12,63-65].

483 Genome-centric metatranscriptomics showed that microbial communities enriched from soil
484 collected at a plastic landfill could actively metabolize PELW as the sole carbon source, whereas
485 no growth was observed in the pristine LDPE (**Fig. S2**). PELW contains shorter hydrocarbons,
486 alkanes and 2-ketones (**Fig. 3**), which serve as substrates for the microbes. [66]. Genes coding for
487 enzymes for terminal oxidation of alkane, including the monooxygenases LadA and AlkB, were
488 upregulated in the S1PELW, S1C30, S2C30 and S2C40 enrichments (**Fig. 2**). In the S2PELW and
489 S1C40 enrichments, upregulated CYP genes may allow subterminal hydroxylation of alkanes (**Fig.**
490 **2C-D**), enabling the microorganisms to degrade alkanes without AlkB or LadA [42]. Notably,
491 several genes encoding FMOs were upregulated on PELW, C30 and C40 (**Fig. 2**). The FMO family
492 comprises a diverse range of xenobiotic-metabolizing enzymes, which use NADPH as a cofactor,
493 and FAD as a prosthetic group. This family includes BVMOs that can also play a role in the
494 subterminal oxidation of alkanes [67]. Here, an alkane monooxygenase introduces a hydroxyl
495 group at a subterminal position of the alkane chain, which is further oxidized to a ketone by an
496 alcohol dehydrogenase. The carbonyl group in the ketone can then converted into an ester group
497 by a BVMO [66]. If these FMOs have BVMO functionality, they can contribute to the conversion of
498 2-ketones, derived from the PELW, or subterminally hydroxylated alkanes, into esters.

499 Following isolation of the dominant species involved in PELW degradation, *A. guillouiae* FS11,
500 proteomics and substrate analyses further demonstrated that it metabolizes the smaller
501 compounds (alkanes and 2-ketones) in the PELW but is not able to cleave the polymeric backbone
502 (**Fig. 4**). Proteomic results revealed that *A. guillouiae* FS11 metabolizes PELW components via
503 terminal alkane oxidation, β-oxidation, and the TCA cycle, with abundant AlkB, LadA, Adh, YiaY,
504 ALDH, and several FMOs, including FMO_2974, uniquely detected in PELW-derived proteomes
505 (**Fig. 5A**). FMOs may actively interact with the 2-ketones and alkanes present in the oxidized
506 PELW via the subterminal oxidation pathway (**Fig. 5B**). The exact role of the putative BVMOs
507 remains to be elucidated through biochemical characterization on these substrates.

508 In summary, our study provides a valuable approach for studying how microbial communities
509 interact with PE and PE-derivatives, and results support two main conclusions. First, advanced
510 substrate characterization before and after microbial growth is essential to convincingly support
511 assumptions of microbes being able to break down the PE backbone and subsequent
512 mineralization. Second, the soil microbial communities and bacterial isolate could efficiently
513 utilize shorter-chain and oxidized-derivatives of PE, while evidence of degradation of longer

514 chain, pristine LDPE was not obtained. These results, in combination with the lack of
515 biochemically characterized enzymes which act on polymeric PE [68], indicate that efforts should
516 be made to create new PE-like materials with oxygen functionality to add enzymatic recyclability.
517 Even though PE in nature remains challenging, our study can help guide the field of microbial
518 plastic degradation by highlighting the challenges associated with data interpretation, and to
519 advise caution in future studies.

520 Acknowledgements

521 This research was funded by the Research Council of Norway under grant agreement no. 326975
522 (Enzyclic project). Mass spectrometry-based proteomic analyses were conducted at the MS and
523 Proteomics Core Facility, Norwegian University of Life Sciences. This facility is a member of the
524 National Network of Advanced Proteomics Infrastructure (NAPI), which is funded by the
525 Research Council of Norway INFRASTRUKTUR-program (project number: 295910). The authors
526 acknowledge Elixir Norway, supported by the Research Council of Norway's (NFR) grant
527 agreement no. 322392, for the data deposition support received for this study.

528 Conflicts of interest

529 The authors declare no conflicts of interest.

530 References

531 1. Sadeghi B, Marfavi Y, AliAkbari R, Kowsari E, Borbor Ajdari F, Ramakrishna S. Recent
532 Studies on Recycled PET Fibers: Production and Applications: a Review. *Materials Circular*
533 *Economy*. 2021/01/22 2021;3(1):4. doi:10.1007/s42824-020-00014-y
534 2. Dokl M, Copot A, Krajnc D, et al. Global projections of plastic use, end-of-life fate and
535 potential changes in consumption, reduction, recycling and replacement with bioplastics to 2050.
536 *Sustainable Production and Consumption*. 2024;51:498-518. doi:10.1016/j.spc.2024.09.025
537 3. Geyer R, Jambeck JR, Law KL. Production, use, and fate of all plastics ever made. *Science*
538 *Advances*. 2017;3(7):e1700782. doi:doi:10.1126/sciadv.1700782
539 4. Geyer R. A Brief History of Plastics. In: Streit-Bianchi M, Cimadevila M, Trettnak W, eds.
540 *Mare Plasticum - The Plastic Sea: Combatting Plastic Pollution Through Science and Art*. Springer
541 International Publishing; 2020:31-47.
542 5. Roychand R, Zafar MA, Jacob M, Ngo T. A Comprehensive Review on the Thermochemical
543 Treatment of Plastic Waste to Produce High Value Products for Different Applications. *Materials*
544 *Circular Economy*. 2025;7(1):3. doi:10.1007/s42824-024-00157-2
545 6. Browning S, Beymer-Farris B, Seay JR. Addressing the challenges associated with plastic
546 waste disposal and management in developing countries. *Current Opinion in Chemical*
547 *Engineering*. 2021;32:100682. doi:10.1016/j.coche.2021.100682
548 7. Schyns ZOG, Shaver MP. Mechanical Recycling of Packaging Plastics: A Review.
549 *Macromolecular Rapid Communications*. 2021;42(3):2000415. doi:10.1002/marc.202000415
550 8. Salinas J, Carpena V, Martínez-Gallardo MR, et al. Development of plastic-degrading
551 microbial consortia by induced selection in microcosms. Original Research. *Frontiers in*
552 *Microbiology*. 2023;14doi:10.3389/fmicb.2023.1143769

9. Giangeri G, Morlino MS, De Bernardini N, et al. Preliminary investigation of microorganisms potentially involved in microplastics degradation using an integrated metagenomic and biochemical approach. *Sci Total Environ*. Oct 15 2022;843:157017. doi:10.1016/j.scitotenv.2022.157017

10. Lyu L, Fang K, Huang X, Tian X, Zhang S. Polyethylene is degraded by the deep-sea *Acinetobacter venetianus* bacterium. *Environmental Chemistry Letters*. 2024;22(4):1591-1597. doi:10.1007/s10311-024-01708-4

11. Nag M, Lahiri D, Dutta B, Jadav G, Ray RR. Biodegradation of used polyethylene bags by a new marine strain of *Alcaligenes faecalis* LNDR-1. *Environmental Science and Pollution Research*. 2021;28(30):41365-41379. doi:10.1007/s11356-021-13704-0

12. Seong HJ, Kim H, Ko Y-J, et al. Enhancing polyethylene degradation: a novel bioprocess approach using *Acinetobacter nosocomialis* pseudo-resting cells. *Applied Microbiology and Biotechnology*. 2024;108(1):1-12. doi:10.1007/s00253-023-12930-5

13. Shovitri M, Nafi'ah R, Antika TR, Alami NH, Kuswytasari ND, Zulaikha E. Soil burial method for plastic degradation performed by *Pseudomonas* PL-01, *Bacillus* PL-01, and indigenous bacteria. *AIP Conference Proceedings*. 2017;1854(1)doi:10.1063/1.4985426

14. Santo M, Weitsman R, Sivan A. The role of the copper-binding enzyme – laccase – in the biodegradation of polyethylene by the actinomycete *Rhodococcus ruber*. *International Biodeterioration & Biodegradation*. 2013;84:204-210. doi:10.1016/j.ibiod.2012.03.001

15. Kim HR, Lee C, Shin H, Kim J, Jeong M, Choi D. Isolation of a polyethylene-degrading bacterium, *Acinetobacter guillouiae*, using a novel screening method based on a redox indicator. *Heliyon*. 2023;9(5)doi:10.1016/j.heliyon.2023.e15731

16. Tao X, Ouyang H, Zhou A, et al. Polyethylene Degradation by a *Rhodococcous* Strain Isolated from Naturally Weathered Plastic Waste Enrichment. *Environmental Science & Technology*. 2023;57(37):13901-13911. doi:10.1021/acs.est.3c03778

17. Skariyachan S, Patil AA, Shankar A, Manjunath M, Bachappanavar N, Kiran S. Enhanced polymer degradation of polyethylene and polypropylene by novel thermophilic consortia of *Brevibacillus* sps. and *Aneurinibacillus* sp. screened from waste management landfills and sewage treatment plants. *Polymer Degradation and Stability*. 2018;149:52-68. doi:10.1016/j.polymdegradstab.2018.01.018

18. Jendrossek D. Polyethylene and Related Hydrocarbon Polymers ("Plastics") Are not Biodegradable. *New Biotechnology*. 2024;doi:10.1016/j.nbt.2024.08.503

19. Cuthbertson AA, Lincoln C, Miscall J, et al. Characterization of polymer properties and identification of additives in commercially available research plastics. *Green Chemistry*. 2024;26(12):7067-7090. doi:10.1039/D4GC00659C

20. Vera-Ponce De León A, Hensen T, Hoetzinger M, et al. Genomic and functional characterization of the Atlantic salmon gut microbiome in relation to nutrition and health. *Nature Microbiology*. 2024;9(11):3059-3074. doi:10.1038/s41564-024-01830-7

21. *Dorado*. 2024. https://github.com/nanoporetech/dorado

22. Newell RJP, Aroney STN, Zaugg J, Sternes P, Tyson GW, Woodcroft BJ. Aviary: Hybrid assembly and genome recovery from metagenomes with Aviary. 2024;doi:10.5281/zenodo.10806928

23. Bowers RM, Kyrpides NC, Stepanauskas R, et al. Minimum information about a single amplified genome (MISAG) and a metagenome-assembled genome (MIMAG) of bacteria and archaea. *Nature Biotechnology*. 2017;35(8):725-731. doi:10.1038/nbt.3893

24. Chaumeil P-A, Mussig AJ, Hugenholtz P, Parks DH. GTDB-Tk v2: memory friendly classification with the genome taxonomy database. *Bioinformatics*. 2022;38(23):5315-5316. doi:10.1093/bioinformatics/btac672

25. Shaffer M, Borton MA, McGivern BB, et al. DRAM for distilling microbial metabolism to automate the curation of microbiome function. *Nucleic Acids Research*. 2020;48(16):8883-8900. doi:10.1093/nar/gkaa621

26. *R: A Language and Environment for Statistical Computing*. 2024. https://www.R-project.org/

27. *ggplot2: Elegant Graphics for Data Analysis*. Springer-Verlag; 2016. https://ggplot2.tidyverse.org
28. *FastQC: A Quality Control Tool for High Throughput Sequence Data*. 2010. http://www.bioinformatics.babraham.ac.uk/projects/fastqc/
29. Chen S, Zhou Y, Chen Y, Gu J. fastp: an ultra-fast all-in-one FASTQ preprocessor. *Bioinformatics*. 2018;34(17):i884-i890. doi:10.1093/bioinformatics/bty560
30. Kopylova E, Noé L, Touzet H. SortMeRNA: fast and accurate filtering of ribosomal RNAs in metatranscriptomic data. *Bioinformatics*. 2012;28(24):3211-3217. doi:10.1093/bioinformatics/bts611
31. Bray NL, Pimentel H, Melsted P, Pachter L. Near-optimal probabilistic RNA-seq quantification. *Nature Biotechnology*. 2016;34(5):525-527. doi:10.1038/nbt.3519
32. *rstatix: Pipe-Friendly Framework for Basic Statistical Tests*. 2023. https://rpkgs.datanovia.com/rstatix/
33. *cowplot: Streamlined Plot Theme and Plot Annotations for 'ggplot2'*. 2024. https://CRAN.R-project.org/package=cowplot
34. *ggrepel: Automatically Position Non-Overlapping Text Labels with 'ggplot2'*. 2024. https://CRAN.R-project.org/package=ggrepel
35. Kong AT, Leprevost FV, Avtonomov DM, Mellacheruvu D, Nesvizhskii AI. MSFragger: ultrafast and comprehensive peptide identification in mass spectrometry–based proteomics. *Nature Methods*. 2017;14(5):513-520. doi:10.1038/nmeth.4256
36. Yu F, Haynes SE, Nesvizhskii AI. IonQuant Enables Accurate and Sensitive Label-Free Quantification With FDR-Controlled Match-Between-Runs. *Molecular & Cellular Proteomics*. 2021;20doi:10.1016/j.mcpro.2021.100077
37. da Veiga Leprevost F, Haynes SE, Avtonomov DM, et al. Philosopher: a versatile toolkit for shotgun proteomics data analysis. *Nature Methods*. 2020;17(9):869-870. doi:10.1038/s41592-020-0912-y
38. Wickham H. *ggplot2: Elegant Graphics for Data Analysis*. Springer-Verlag; 2016.
39. Abramson J, Adler J, Dunger J, et al. Accurate structure prediction of biomolecular interactions with AlphaFold 3. *Nature*. 2024;630(8016):493-500. doi:10.1038/s41586-024-07487-w
40. Van Kempen M, Kim SS, Tumescheit C, et al. Fast and accurate protein structure search with Foldseek. *Nature Biotechnology*. 2024;42(2):243-246. doi:10.1038/s41587-023-01773-0
41. Meng EC, Goddard TD, Pettersen EF, et al. UCSF ChimeraX: Tools for structure building and analysis. *Protein Science*. 2023;32(11)doi:10.1002/pro.4792
42. Van Bogaert INA, Groeneboer S, Saerens K, Soetaert W. The role of cytochrome P450 monooxygenases in microbial fatty acid metabolism. *The FEBS Journal*. 2011;278(2):206-221. doi:10.1111/j.1742-4658.2010.07949.x
43. Kim Y-J, Lee J-S, Park J-A, Kim H-O, Lim KS, Ha S-J. Biodegradation of Low-Density Polyethylene by *Acinetobacter guillouiae* PL211 Isolated from the Waste Treatment Facility. *Microbiology and Biotechnology Letters*. 2024;52(2):189-194. doi:10.48022/mbl.2404.04005
44. Rong Z, Xu X-W, Wu Y-H. Biodegradation of low-density polyethylene film by two bacteria isolated from plastic debris in coastal beach. *Ecotoxicology and Environmental Safety*. 2024;278:116445. doi:10.1016/j.ecoenv.2024.116445
45. Tarafdar A, Lee J-U, Jeong J-E, et al. Biofilm development of *Bacillus siamensis* ATKU1 on pristine short chain low-density polyethylene: A case study on microbe-microplastics interaction. *Journal of Hazardous Materials*. 2021;409:124516. doi:10.1016/j.jhazmat.2020.124516
46. Rong Z, Ding Z-H, Wu Y-H, Xu X-W. Degradation of low-density polyethylene by the bacterium *Rhodococcus* sp. C-2 isolated from seawater. *Science of The Total Environment*. 2024;907:167993. doi:10.1016/j.scitotenv.2023.167993
47. Kim Y-J, Kim Y-H, Shin Y-R, et al. Efficient biodegradation of low-density polyethylene by *Pseudomonas plecoglossicida* SYp2123 was observed through FT-IR and FE-SEM analysis. *Biotechnology and Bioprocess Engineering*. 2024;29(4):743-750. doi:10.1007/s12257-024-00108-3

48. Kim HR, Lee YE, Suh D-E, Choi D, Lee S. Multistep Enzymatic Low-density Polyethylene Degradation via Phenylalanine Monooxygenase and Isocitrate Lyase in *Pseudomonas aeruginosa*. American Chemical Society (ACS); 2024.
49. Zampolli J, Mangiagalli M, Vezzini D, et al. Oxidative degradation of polyethylene by two novel laccase-like multicopper oxidases from *Rhodococcus opacus* R7. *Environmental Technology & Innovation*. 2023;32:103273. doi:10.1016/j.eti.2023.103273
50. Zampolli J, Orro A, Manconi A, Ami D, Natalello A, Di Gennaro P. Transcriptomic analysis of *Rhodococcus opacus* R7 grown on polyethylene by RNA-seq. *Scientific Reports*. 2021;11(1)doi:10.1038/s41598-021-00525-x
51. Yin CF, Xu Y, Li T, Zhou NY. Wide distribution of the *sad* gene cluster for sub‐terminal oxidation in alkane utilizers. *Environmental Microbiology*. 2022;24(12):6307-6319. doi:10.1111/1462-2920.16124
52. Yin C-F, Nie Y, Li T, Zhou N-Y. AlmA involved in the long-chain n-alkane degradation pathway in *Acinetobacter baylyi* ADP1 is a Baeyer–Villiger monooxygenase. *Applied and Environmental Microbiology*. 2024;90(1)doi:10.1128/aem.01625-23
53. Sanluis-Verdes A, Colomer-Vidal P, Rodriguez-Ventura F, et al. Wax worm saliva and the enzymes therein are the key to polyethylene degradation by *Galleria mellonella*. *Nature Communications*. 2022;13(1)doi:10.1038/s41467-022-33127-w
54. Zhang Z, Peng H, Yang D, Zhang G, Zhang J, Ju F. Polyvinyl chloride degradation by a bacterium isolated from the gut of insect larvae. *Nature Communications*. 2022;13(1)doi:10.1038/s41467-022-32903-y
55. Stepnov AA, Lopez-Tavera E, Klauer R, et al. Revisiting the activity of two poly(vinyl chloride)- and polyethylene-degrading enzymes. *Nature Communications*. 2024;15(1)doi:10.1038/s41467-024-52665-z
56. Wei R, Weber G, Blank LM, Bornscheuer UT. Process insights for harnessing biotechnology for plastic depolymerization. *Nature Chemical Engineering*. 2025;2(2):110-117. doi:10.1038/s44286-024-00171-w
57. Oiffer T, Leipold F, Süss P, et al. Chemo‐Enzymatic Depolymerization of Functionalized Low‐Molecular‐Weight Polyethylene. *Angewandte Chemie International Edition*. 2024;63(50)doi:10.1002/anie.202415012
58. Suresh B, Maruthamuthu S, Khare A, et al. Influence of thermal oxidation on surface and thermo-mechanical properties of polyethylene. *Journal of Polymer Research*. 2011/11/01 2011;18(6):2175-2184. doi:10.1007/s10965-011-9628-0
59. Therias S, Rapp G, Masson C, Gardette J-L. Limits of UV-light acceleration on the photooxidation of low-density polyethylene. *Polymer Degradation and Stability*. 2021/01/01/ 2021;183:109443. doi:https://doi.org/10.1016/j.polymdegradstab.2020.109443
60. Li YP, Pan JC, Ma YL. Elucidation of multiple alkane hydroxylase systems in biodegradation of crude oil n‐alkane pollution by *Pseudomonas aeruginosa* DN1. *Journal of Applied Microbiology*. 2020;128(1):151-160. doi:10.1111/jam.14470
61. Liu H, Xu J, Liang R, Liu J. Characterization of the Medium- and Long-Chain n-Alkanes Degrading *Pseudomonas aeruginosa* Strain SJTD-1 and Its Alkane Hydroxylase Genes. *PLoS ONE*. 2014;9(8)doi:10.1371/journal.pone.0105506
62. Maeng JH, Sakai Y, Tani Y, Kato N. Isolation and characterization of a novel oxygenase that catalyzes the first step of n-alkane oxidation in *Acinetobacter* sp. strain M-1. *Journal of Bacteriology*. 1996;178(13):3695-3700. doi:10.1128/jb.178.13.3695-3700.1996
63. Jeon HJ, Kim MN. Functional analysis of alkane hydroxylase system derived from *Pseudomonas aeruginosa* E7 for low molecular weight polyethylene biodegradation. *International Biodeterioration & Biodegradation*. 2015;103:141-146. doi:10.1016/j.ibiod.2015.04.024
64. Shilpa, Basak N, Meena SS. Biodegradation of low-density polythene (LDPE) by a novel strain of *Pseudomonas aeruginosa* WD4 isolated from plastic dumpsite. *Biodegradation*. 2024;35(5):641-655. doi:10.1007/s10532-023-10061-2

65. Zhang H, Lu Y, Wu H, Liu Q, Sun W. Effect of an *Acinetobacter pittobacter* on low-density polyethylene. *Environmental Science and Pollution Research*. 2022;30(4):10495-10504. doi:10.1007/s11356-022-22658-w

66. Ji Y, Mao G, Wang Y, Bartlam M. Structural insights into diversity and n-alkane biodegradation mechanisms of alkane hydroxylases. *Frontiers in Microbiology*. 2013;4doi:10.3389/fmicb.2013.00058

67. Ceccoli RD, Bianchi DA, Fink MJ, Mihovilovic MD, Rial DV. Cloning and characterization of the Type I Baeyer–Villiger monooxygenase from Leptospira biflexa. *AMB Express*. 2017;7(1)doi:10.1186/s13568-017-0390-5

68. Buchholz PCF, Feuerriegel G, Zhang H, et al. Plastics degradation by hydrolytic enzymes: The plastics‐active enzymes database—PAZy. *Proteins: Structure, Function, and Bioinformatics*. 2022;90(7):1443-1456. doi:10.1002/prot.26325

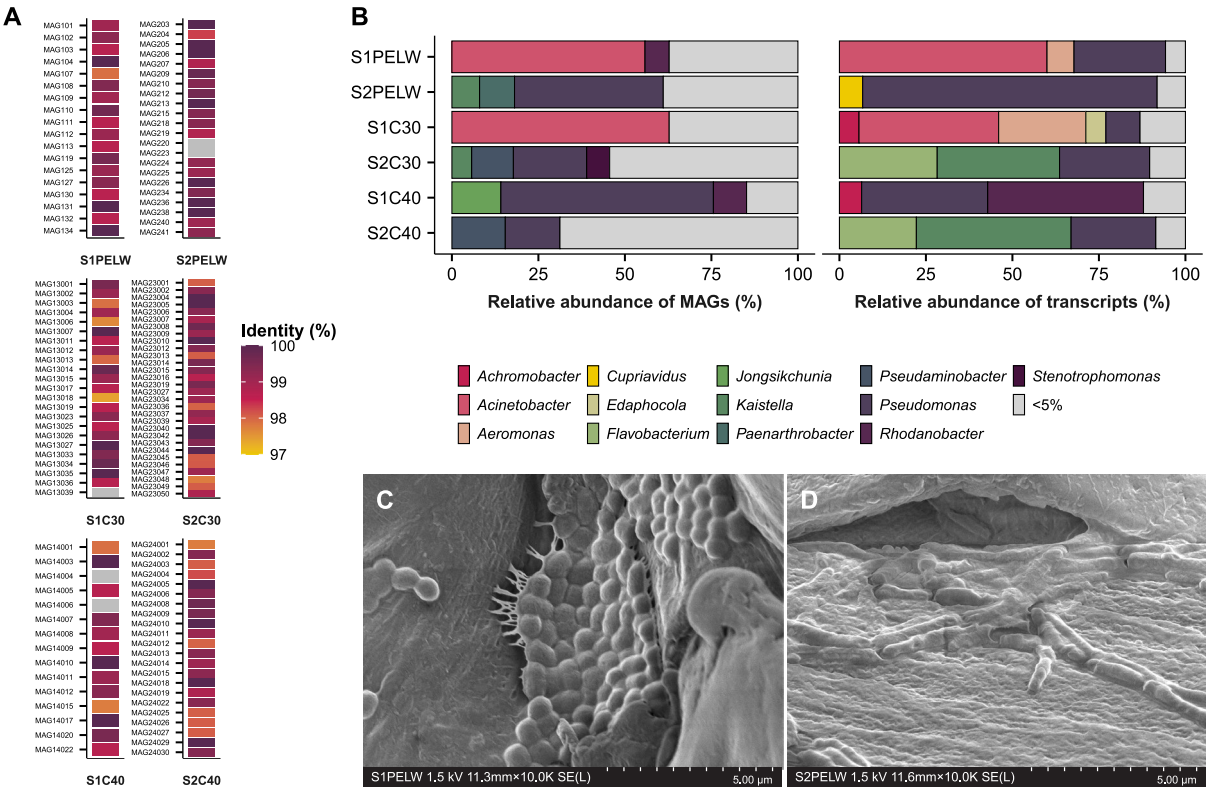

Fig. 1. Relative abundance and activity of MAGs in the PELW, triacontane (C30) and tetracontane (C40) enrichment cultures as well as their detection in the original soil communities. **(A)** A list of high- and medium-quality MAGs reconstructed from the different enrichment cultures and their identification in the original S1 and S2 soil communities. The detection is based on the alignment of 16S rRNA gene sequence of each individual MAG to the OTUs in S1 and S2. The 16S rRNA gene detection is colored based on the % identity of the gene alignment. At a 97% identity level to OTUs, 96% of the MAGs were detected in the soil samples. **(B)** Relative abundance of MAGs (grouped at genus level) in each enrichment and the relative abundance of total transcripts per million (TPM) for each MAG within each community. Genera with a relative abundance of <5% are grouped together. Panels **(C)** and **(D)** show SEM images of the PELW surface following growth with the S1PELW and S2PELW communities, respectively. Each community exhibits a distinct morphology of bacteria attached to the PELW surface.

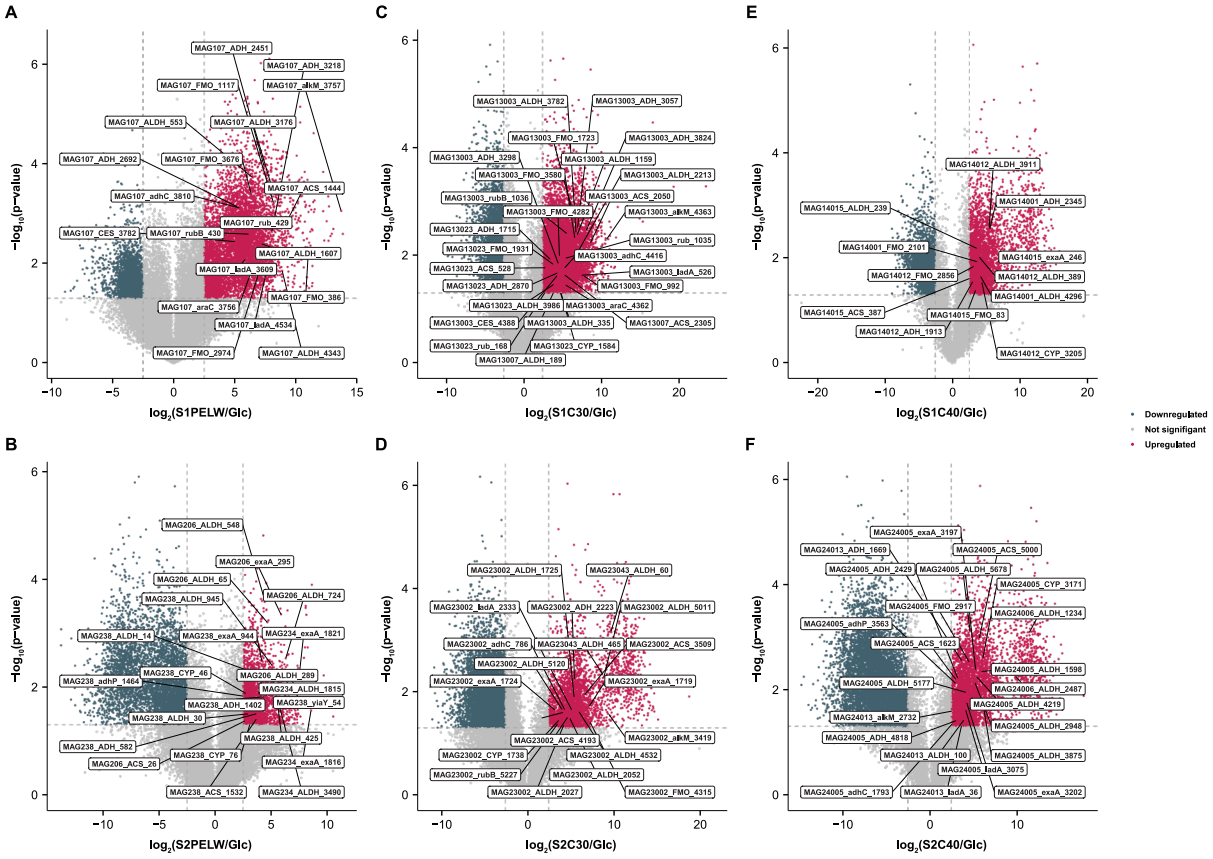

Fig. 2. Volcano plot indicating different transcripts in the PELW, triacontane (C30) and tetracontane (C40) degrading communities that displayed a large magnitude of fold-changes in TPM and high statistical significance (-$\log_{10}$ of p-values, t-test) compared to the same communities grown on glucose. Panel **(A)** and **(B)** display upregulated genes in the S1PELW and S2PELW tertiary communities, respectively. Panel **(C)** and **(D)** show upregulated genes in the S1C30 and S2C30 tertiary communities, respectively. Panel **(E)** and **(F)** show the upregulated genes in the S1C40 and S2C40 tertiary communities, respectively. KEGG Orthology IDs were used to identify and highlight genes known to be involved in alkane degradation, 2-ketone degradation and β-oxidation of fatty acids. The dashed horizontal line denotes the p-value cut-off ($p < 0.05$), and the dashed vertical lines denote the $\log_2$-fold change cut-off (< -2.5 and > 2.5). Source data are provided in Table S1B-G.

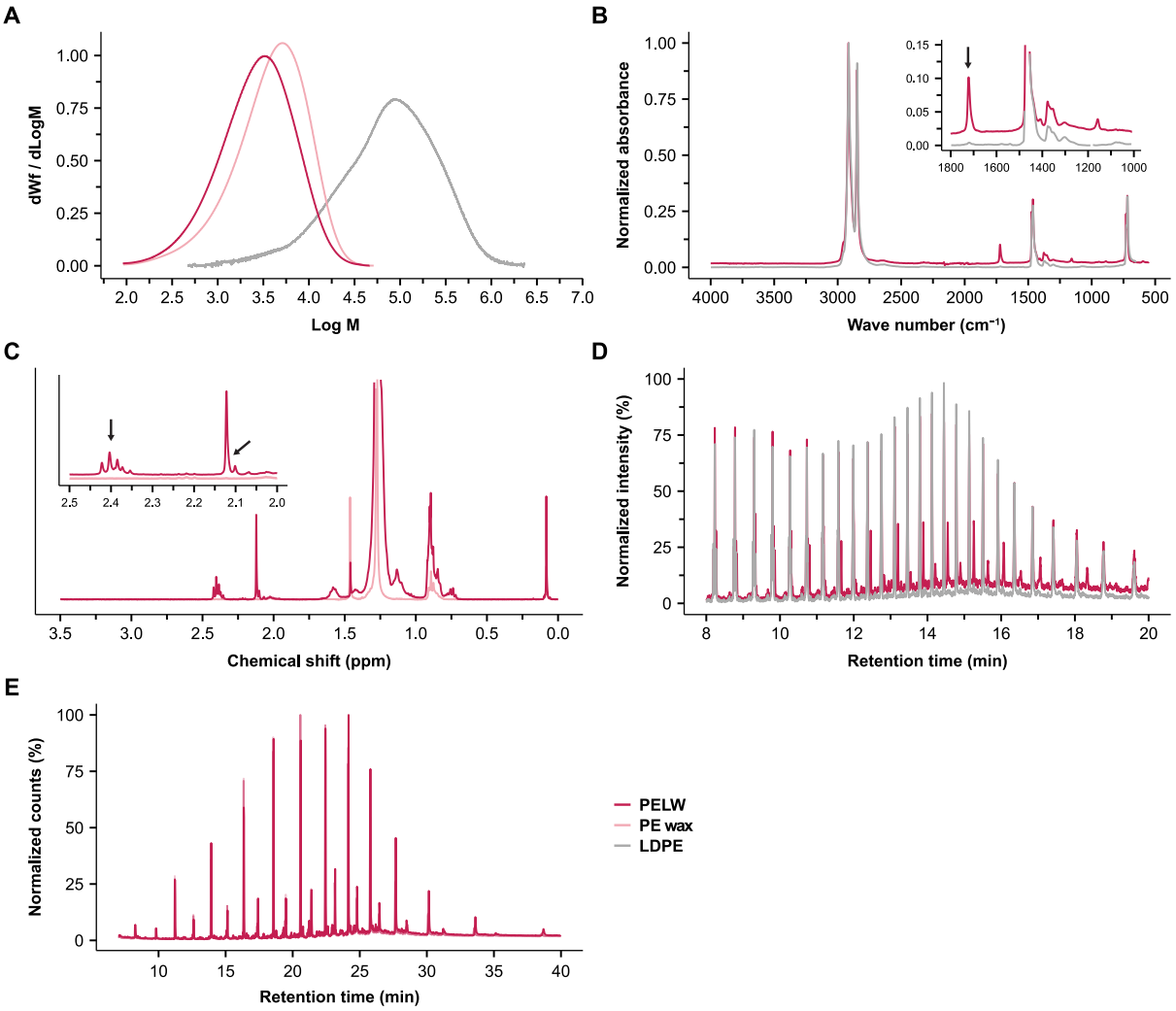

Fig. 3. Characterization of PELW. Data for reference LDPE was obtained from Stepnov et al. [56]. **(A)** SEC analysis of PELW, a reference LDPE and a PE wax. The molar mass distribution of PELW is different than that of the PE wax and LDPE. **(B)** Overlayed FTIR spectra of the PELW and a reference LDPE. Compared to LDPE, the strong additional peak at ≈1722 cm^{-1} clearly indicates oxygen functionalities in the PELW (i.e. carbonyl groups in ketones or aldehydes). **(C)** NMR spectra of PELW. The singlets at 2.10-2.12 ppm and the triplet between 2.35-2.42 ppm confirm the presence of a carbonyl at the second carbon. **(D)** Overlaid Py-GC-MS chromatograms of PELW and LDPE. In the PELW, additional peaks were observed that were absent in the LDPE (see Table S2D for peak annotation). **(E)** GC-MS chromatograms of PELW ethyl acetate extracts, showing alkanes and 2-ketones between 10-35 carbons in chain length (see Table S2E for peak annotations). Reference LDPE data for panel **A** and **B** were obtained from Stepnov et al. [56]. Source data can be found in Table S2A-E.

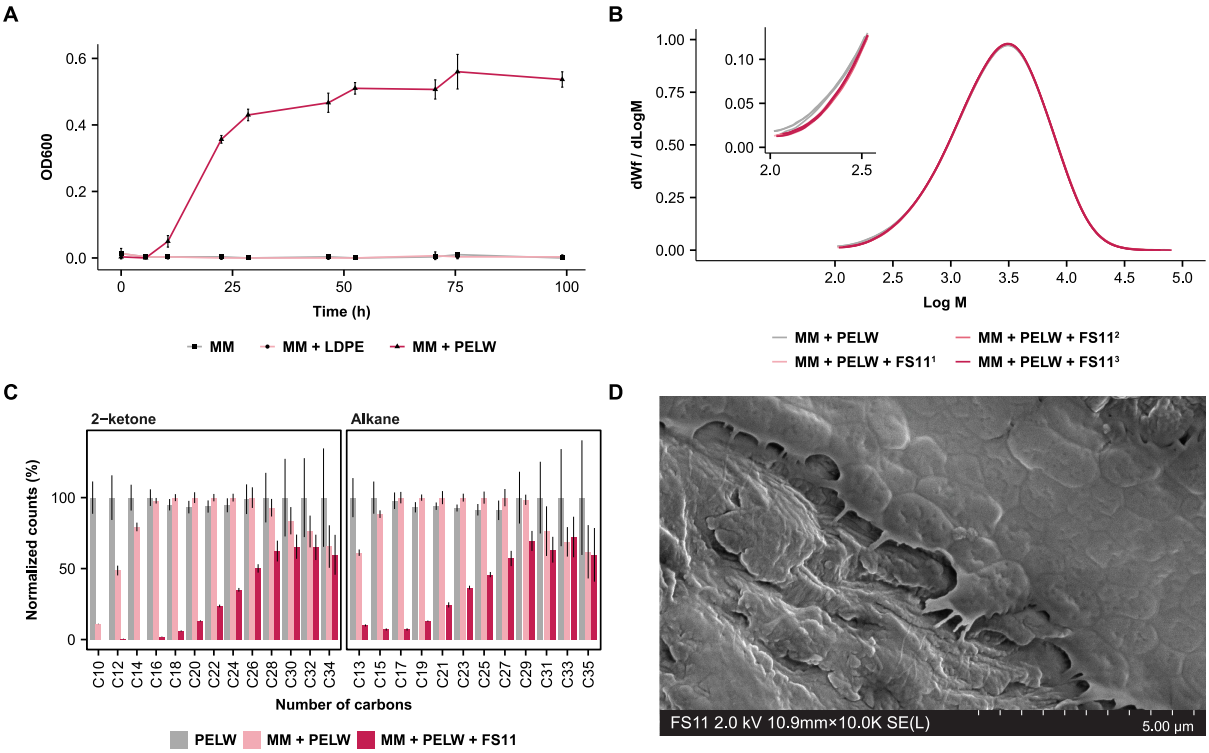

Fig. 4. Growth profiles of *A. guillouiae* FS11 on PELW and subsequent characterization of the substrate. **(A)** Growth of A. guillouiae FS11 in minimal medium without any carbon source (MM) or supplemented with either PELW (MM+PELW) or LDPE (MM+LDPE). Data are averages ± standard deviations (error bars) of three biological replicates. **(B)** SEC chromatograms of PELW following incubation with MM or MM + *A. guillouiae* FS11. One control sample (MM + PELW) and three replicates (MM + PELW + FS11$^{1\text{-}3}$) were set up. Sample-specific chromatograms are shown. Note that chromatograms are superimposing in the high molecular weight regions, indicating no degradation of polymeric fraction of PELW substrate, as the molar mass distribution would shift to the left. **(C)** GC-MS results of PELW showing the relative reduction of each compound after growth of *A. guillouiae* FS11. Compound loss is expressed relative to the amount of the same compound detected in PELW incubated in the absence of *A. guillouiae* FS11. **(D)** SEM image of *A. guillouiae* FS11 adhering to the surface of PELW. Source data for SEC and GC-MS can be found in Table S2F-G.

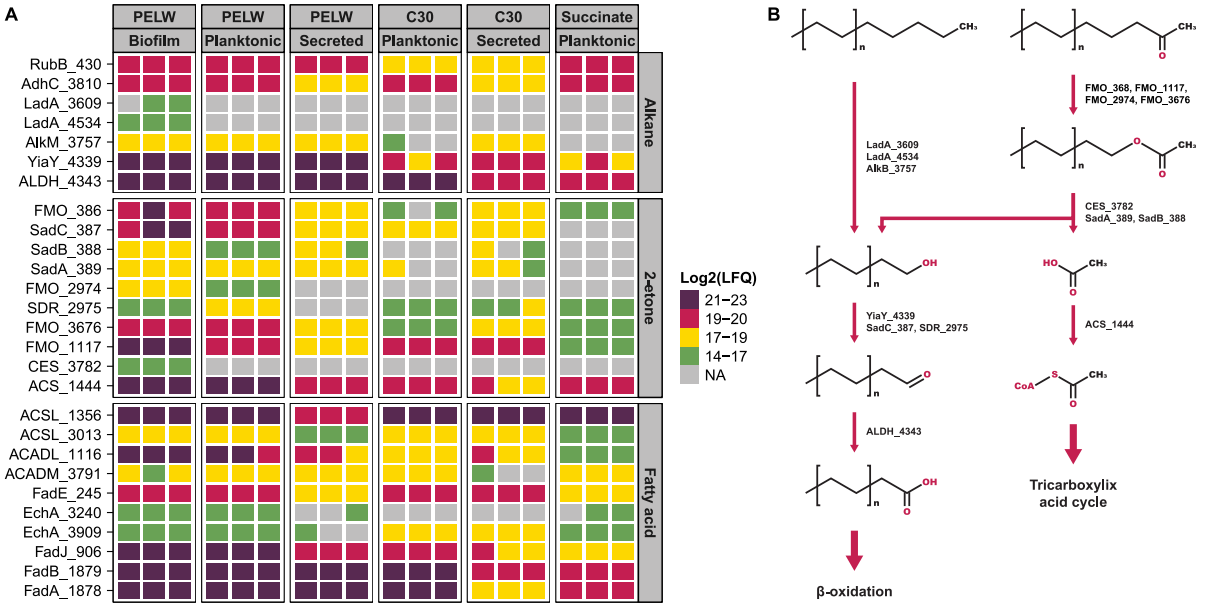

Fig. 5. Selected differentially abundant proteins in the *A. guillouiae* FS11 proteome and proposed metabolic pathway for degradation of 2-ketones and alkanes in PELW. Panel A shows the LFQ intensities of the known and proposed enzymes in the pathways for terminal alkane oxidation, 2-ketone degradation and β-oxidation. Missing values are shown in grey. Panel B shows a proposed metabolic pathway of alkanes and 2-ketones found in PELW, with chain lengths between 10-35. Alkanes are terminally oxidized, while 2-ketones are oxidized by FMOs, generating esters. Esters are hydrolyzed into alcohols and acetate, which can enter the alkane degradation pathway and the tricarboxylic acid (TCA) cycle, respectively.